Hybrid State Feedback Position-Force Control of Hydraulic Cylinder

Philipp Pasolli
University of Agder (UiA)
Faculty of Engineering and Science
Post box 422, 4604-Kristiansand, Norway
philipp.pasolli@uia.no

Michael Ruderman
University of Agder (UiA)
Faculty of Engineering and Science
Post box 422, 4604-Kristiansand, Norway
michael.ruderman@uia.no

Abstract—**A hybrid position-force control is proposed using a unified state feedback controller in combination with feed-forward dead-zone compensation. Dead-zone compensator was constructed as inverse of the identified static map while the state feedback gains were obtained using a numerical optimization routine. An accurate state-space model affine in states and control, derived in a previous work, was used for closed-loop simulations and control tuning. A trigger event for automatic switching between position and force control was defined and integrated into overall control architecture alongside with a feed-forward low-pass filter reducing high frequency components in the control signal. Experimental evaluations were performed for different references with automatic switching between the position trajectory following and force set value regulation.**

I. Introduction

Hydraulic systems are widely used in various industries due to their longevity, compactness, modularity and excellent power to mass ratio. Further they have the ability of holding large forces constantly without overheating, as most other actuators would. However, hydraulic systems contain multiple nonlinearities e.g. in the orifice equations, mechanical friction, leakage, and others, which either can not be modeled completely or require some in depth investigation to come up with a proper modeling solution. On top of that, there are uncertain model properties e.g. wear of components, bulk modulus, and others which make hydraulic systems not only more challenging to model but also to control.

In several cases of hydraulic applications a lot of tasks are highly repetitive and tedious e.g. in excavators, while still being controlled manually by operators. While at least as semi-automatic control already entered these application fields, it is still the standard PID controllers which are regulation most of the closed-loops. Some optimal control designs for PID, with additional nonlinear extensions, were reported e.g. [1] for improving the the control system performance. In other motion control researches, different types of controllers, like adaptive, extended state-feedback and variable structure, are shown as superior to the standard PID, not just for hydraulic systems, cf. [2]–[5].

Keeping in mind an example with excavator, it could be destructive for equipment to run with position control only, so that a force control approach might be required. Such control approaches are, however, especially challenging if an environment has uncertainties in resistive force and either an alternative control strategy or a kind universal controller with relatively wide operational range is needed. For several force control strategies, including those designed for hydraulic systems, we refer to [6]–[9]. Yet if a fully automated system is desired, a combination of position and force control should be sought, capable of utilizing both types of controllers depending on the environmental factors. Such hybrid control approaches are quite common and continue to be a field of intense research especially in robotics, cf. [10]–[12].

In this paper a hybrid position and force control is pursued based on an integral state feedback controller, see e.g. [13] for overview. While for position control the system can basically be regulated using a PID, for a force control is is a pressure feedback which becomes vital for actively damping the system, cf. [14]. Other research showed that a pressure feedback control can also be implemented directly using additional hardware, cf. [15].

For laying out a proper control architecture, a detailed model of the system is required. In [16] a reduced hydraulic model in approach to our test setup is described which was expanded upon in [17] by linearizing it and creating a state-space model affine in both control and states. The proposed hybrid position-force control is based on the latter. The rest of the paper is structured as follows. In section II the modeling from previous work [17] is revised and summed up while introducing the integral state feedback controller in section III. Section IV evaluates the measurements performed and in V a summary of the work is given.

II. System Modeling

The hydraulic system modeled is a single rod, double acting cylinder attached to a servo valve connected to a HPU (Hydraulic Power Unit). Characteristics of both the valve and the cylinder were previously identified in [17]. Simulations and measurements were compared verifying the model and its identified parameters, including a dead-zone-saturation combination, the valves dynamics as a second-order system, orifice and continuity equations and the Stribeck friction model for cylinder. For the model reduction the assumption of equal cross sectional areas of the cylinder was made, therefore introducing a load dependent pressure, and

simplifying both the orifice and continuity equations. Also, the valves' dynamics was neglected due to an observed unity gain and negligible phase lag in the frequency range of interest. Linearizations of type $y = kx + d$, i.e. with slope k and offset d, were performed for the identified nonlinearities, therefore resulting in a state-space model affine in control and states.

For this work, the state-space model was expanded by an event switching between the position and force control, denoted by h. Expanding the state vector for state feedback control with integral term results in the following formulation

$$\dot{\mathbf{x}} = \mathbf{A}(\mathbf{x}, h)\mathbf{x} + \mathbf{b}(\mathbf{x})r(h) + \mathbf{f}, \qquad (1)$$
$$y = \mathbf{c}(h)^T\mathbf{x}, \qquad (2)$$

The state vector is given by $\mathbf{x} = [x, \dot{x}, P_L, F_L, e]$ where e is the error between reference and measured output (position or force), x is the cylinder's position, $\dot{x}$ the relative velocity, P_L the load-dependent pressure and F_L is the load force. The introduction of h and switching between control schemes leads inherently to a change of the system dynamics and, therefore, to two different system matrices $\mathbf{A}$ and output vectors $\mathbf{c}$, depending on the instantaneous control mode. r is the corresponding reference signal, again dependent on h. $\mathbf{b}$ is the input coupling vector and $\mathbf{f}$ is correspondingly the affine term, cf. [17].

III. CONTROL DESIGN

This section describes the single steps of designing the closed-loop control system, its parameter optimization, definition of the switching event, static dead-zone compensator, and feed-forward filter for the control signal.

A. Static dead-zone compensation

The valve to be controlled contains a dead-zone-saturation combination. While the saturation only limits the maximum output values, the dead-zone affects the valve's behavior around its origin in the range of $\pm 10\%$ of the valves command, thus directly influencing the closed-loop behavior. To overcome this issue a static dead-zone compensation is introduced. This is done by flipping the identified dead-zone of the system over a slope with unity gradient, so as to achieve best possible compensation results, cf. Fig. 1. The static compensator
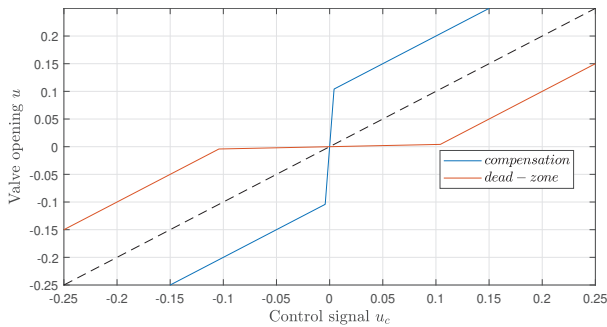

Fig. 1: Static dead-zone compensation

function is then linearized resulting in 3 linearisation regions described by

$$u = k_a u_c + d_a, \qquad (3)$$

where u_c is the control signal and u the input to the valve. The corresponding linearization regions (further denoted as cells) are indexed by a.

B. Integral error state-feedback control

After feed forward compensating the dead-zone of the valve, a controller was designed to follow the desired reference for each control strategy, resulting in a state feedback controller

$$u_c = -\mathbf{K}(h)\mathbf{x} \qquad (4)$$

with $\mathbf{K} = [K_1, K_2, K_3, K_4, K_i]$ to be the vector of control gains, determined separately for position ($h = -1$) and force ($h = 1$) control modes. Implementing the proposed controller results in the overall structure shown in Fig. 2, where γ is the static dead-zone compensator.
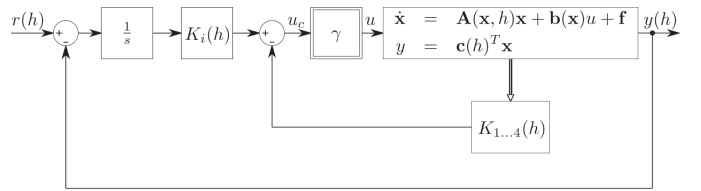

Fig. 2: Control Structure

The matrix and vectors of (1) and (2) are given by

$$\mathbf{A}(h) = \begin{pmatrix} 0 & 1 & 0 & 0 & 0 \\ 0 & -\dfrac{k_w}{m} & \dfrac{\bar{A}}{m} & -\dfrac{1}{m} & 0 \\ a_{31} & a_{32} & a_{33} & a_{34} & a_{35} \\ 0 & 0 & 0 & 0 & 0 \\ -1 & 0 & 0 & 0 & 0 \end{pmatrix}, \quad h = -1$$

$$\mathbf{A}(h) = \begin{pmatrix} 0 & 1 & 0 & 0 & 0 \\ 0 & -\dfrac{k_w}{m} & \dfrac{\bar{A}}{m} & -\dfrac{1}{m} & 0 \\ a_{31} & a_{32} & a_{33} & a_{34} & a_{35} \\ 0 & c & 0 & 0 & 0 \\ 0 & 0 & 0 & -1 & 0 \end{pmatrix}, \quad h = 1 \qquad (5)$$

with the coefficients given by

$$a_{31} = -\frac{4Ek_gk_aK_1}{V_t}\left(k_nP_L^2 + d_nP_L + k_oP_L + d_o\right)$$

$$a_{32} = -\frac{4E}{V_t}\left(k_gk_aK_2(k_nP_L^2 + d_nP_L + k_oP_L + d_o) + \bar{A}\right)$$

$$a_{33} = \begin{aligned}&\frac{4E}{V_t}\big(-k_gk_aK_3(k_nP_L^2 + d_nP_L + k_oP_L + d_o)\\ &\quad +k_o(k_gd_a + d_g) + d_g(k_nP_L + d_n)\\ &\quad +k_gd_a(k_nP_L + d_n) - C_L\big)\end{aligned}$$

$$a_{34} = -\frac{4Ek_gk_aK_4}{V_t}\left(k_nP_L^2 + d_nP_L + k_oP_L + d_o\right)$$

$$a_{35} = \frac{4Ek_gk_aK_i}{V_t}\left(k_oP_L + d_0 + k_nP_L^2 + d_nP_L\right)$$

(6)

with the rest of the vectors described by:

$$\mathbf{b} = \begin{pmatrix} 0 \\ 0 \\ 0 \\ 0 \\ 1 \end{pmatrix}$$

(7)

$$\mathbf{f} = \begin{pmatrix} 0 \\ -\dfrac{d_w}{m} \\ \dfrac{4E(k_gd_od_a + d_od_g)}{V_t} \\ 0 \\ 0 \end{pmatrix}$$

(8)

$$\mathbf{c}(h)^T = \begin{pmatrix} 1 & 0 & 0 & 0 & 0 \end{pmatrix}, \quad h = -1;$$

$$\mathbf{c}(h)^T = \begin{pmatrix} 0 & 0 & 0 & 1 & 0 \end{pmatrix}, \quad h = 1;$$

(9)

In the above equations, E describes the bulk modulus of the hydraulic fluid with V_t being the sum of volumes in the lines from the valve to the cylinder. $\bar{A}$ is the averaged cross section of cylinder, m is the lumped mass moved in the system, and c is the spring constant of a *hard stop* against environment when the system is operated with force control. k and d with the corresponding indices refer to the different cells of linearization of the state space, cf. with (3). C_L is the leakage coefficient between both cylinder chambers.

C. Filtering of control signal

High frequency components were observed in the valve response. This is directly related to the amplification of the noisy sensor signals. While the integrator smoothes the noise out, the state feedback control terms amplify the noise afflicted signals, thus resulting in a high frequency control signal feeded to the valve. While the fast servo-valve is able to follow the reference, such high frequencies on the command signal are not desired, introducing unnecessary wear for the component. An analysis of the control signal showed, that the valve mainly operates at around 25% of its maximum opening which corresponds, according to the measured FRF, to a cutoff

frequency of about $100Hz$. Therefore, a second-order low-pass filter with a cut-off frequency of $100Hz$ was inserted after the dead-zone compensation. This aims filtering out the higher frequencies of the control signal, while not slowing down the overall system dynamics.

D. Event-based switching

For the system to automatically switch between the position and force control a switching event h had to be defined. The system starts at $t = 0s$ with $x = 0$ and $\dot{x} = 0$ with position control of following a given reference, in this case a ramp function, until it reaches a mechanical hard stop that should trigger switching from position to the force control and, correspondingly, reset the integral error. The event trigger is then the load force surpassing a predefined threshold. Analysis of sensor's signal showed that due to the noise, the force peaks of up to $1500N$ in either direction can be observed on top of the current value. Unsuitable threshold definition, therefore, could lead to a limit cycle behavior of periodically switching from force to position control and vice versa. To overcome this issue a delayed relay was introduced, defined by [18]

$$h(t) = \min[\text{sign}(F_H - \beta), \max[h(t_-), \text{sign}(F_H - \alpha)]] \quad (10)$$

with the initial state

$$h(t_0) = \begin{cases} \text{sign}(F_H(t_0)) & \text{if } F_H(t_0) \in (-\infty, \beta) \vee (\alpha, \infty) \\ [-1, +1] & \text{otherwise} \end{cases}$$

(11)

The previous to switching time instance is denoted by t_-, while the assigned parameters are $\alpha = 1500N$, $\beta = -1500N$, and the relay's input value is assigned to be $F_H = F_L - 2000N$.

While the test setup has a mechanical hard stop which introduces a rapid increase of the measured force and therefore triggers switching between the controllers, in the simulation an artificial hard stop was created to verify the control functionality. The hard stop is modeled as a high stiffness spring, without damping, based on the Youngs' modulus equation. Rearranging the equation leads to the spring constant

$$\frac{E_sA_s}{L_0} = \frac{F_L}{\Delta L} = c,$$

(12)

where $E_s = 210GPa$ is the Youngs' modulus of steel, A_s is the cross section of the "spring", L_0 its non deformed length, ΔL the deformation, and F_L the loads force. As can be seen, $F_L/\Delta L$ is equal to c and therefore only E_s, A_s and L_0 are needed for calculating the spring constant.

In the experimental setup, see further in section IV, the hard stop is reached once the left cylinder is fully retracted. The I-beam the cylinders are mounted to, cf. Fig. 5, is assumed to be much stiffer than the combination of cylinder rods plus force sensor and therefore $L_0 = 0.88m$, being the summed length of both cylinder rods and force sensor, is assumed. While there are various components in that chain, $A_s = 5e^{-4}m^2$ was assumed to be uniform and given by the cylinders cross section, leading to a spring constant of $c = 1.2e^8N/m$.

E. Optimal state feedback

For the designed control structure, the state feedback gains are determined as follows. A set of initial gain values was empirically determined first as a starting point for optimization. Different cost functions were assumed for each controller to achieve the desired outcome.

For position control, the cost function is given by

$$\min \int ((r - x)t + u_d t)^2 dt \tag{13}$$

with r being a ramp reference with a slope of $0.05 m/s$, x the cylinder's position and u_d the difference between the control signal after dead-zone compensation and the signal after saturation of the valve. This is included to minimize not only the control error, but also the amount of control signals exceeds the maximum command input admissible by the valve. Multiplications with the time t were performed to punish deviations from the reference harder with increasing time. The initial set of the gain values is was $[50, 0.001, 1e^{-8}, 1e^{-6}, 5000]$. The convergence of the normalized gain values and the cost function are shown in Fig. 3.
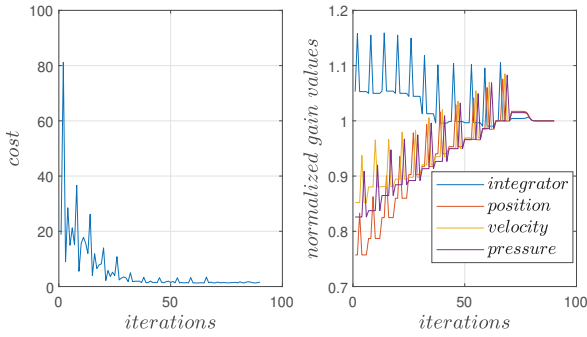

Fig. 4: Cost and gaine value convergence for force control from (14)

TABLE I: Optimized gain values for position and force control

Gain parameter	Position control	Force control
K_i	$5e^3$	0.0014
K_1	73.3	0
K_2	$9e^{-4}$	$3.1e^{-4}$
K_3	$1.65e^{-8}$	$5e^{-8}$
K_4	0	$2.5e^{-9}$

Fig. 3: Cost and gain value convergence for position control from (13)

The cost function for the force control is given by

$$min \int ((r - F_L)t)^2 dt. \tag{14}$$

where r is the reference force defined to be $3500N$ and F_L is the measured load force. Again the difference is multiplied by time to punish deviations from the reference harder with increasing time. Initial values for parameters were taken from previous measurements to be close as possible to the real conditions. The initial set of gain values was $\mathbf{K} = [6e^{-7}, 3e^{-4}, 5e^{-8}, 2e^{-5}, 1.4e^{-3}]$; this was determined empirically. The convergence of the gain values and minimization function are shown in Fig. 4.

Note that K_4 was set to zero for position control because there is no external force acting against the cylinders movement. For the force control, K_1 was set to zero because there is only negligible micro-movement once the hard stop is reached. The optimized values for the control gains are shown in Table I.
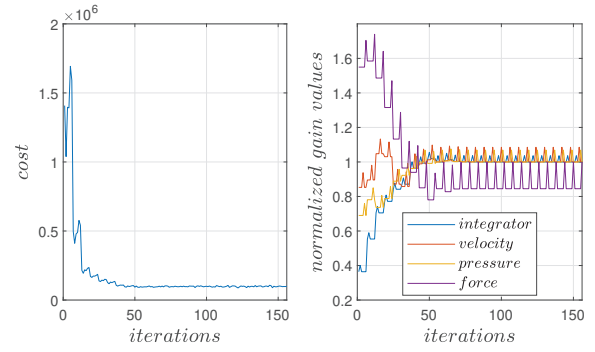
IV. EXPERIMENTAL EVALUATION

The experimental setup used in this work is shown in Fig. 5, where the right cylinder-valve combination is to be controlled, while the force sensor is connecting both cylinders. A hard stop is reached by extending the right cylinder until the left cylinder is fully retracted. More details on the developed setup can be found in [17].
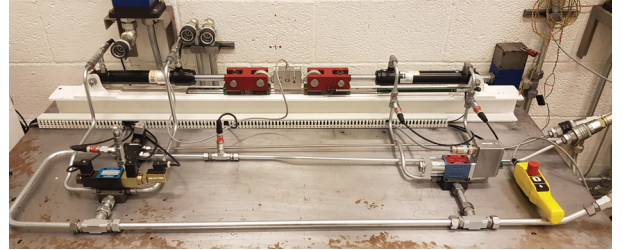

Fig. 5: Experimental setup of hydraulic cylinders

After confirming with simulations that the obtained control parameters lead to the desired system behavior, experiments on the laboratory setup were performed. For position control, the system was supposed to follow two different slopes of $0.03 m/s$ and $0.07 m/s$ starting from a fully retracted position, i.e. $x_0 = 0$, $\dot{x}_0 = 0$, while the reference values for force control are $3500N$ and $7000N$ correspondingly. The measured values for the ramp with slope of $0.03 m/s$ and reference force of $3500N$ are shown in Figs. 6 and 7, while the measured position and force for the slope of $0.07 m/s$ and reference force of $7000N$ are shown in Figs. 8 and 10.

As can be seen from the figures, the cylinder follows the reference position closely for both ramps until reaching the hard stop at a position of about $x_s = 0.11m$ when a rapid
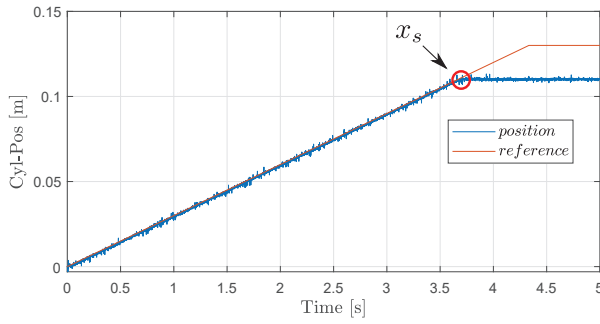
Fig. 6: Measured cylinder position and reference for ramp with 0.03m/s slope
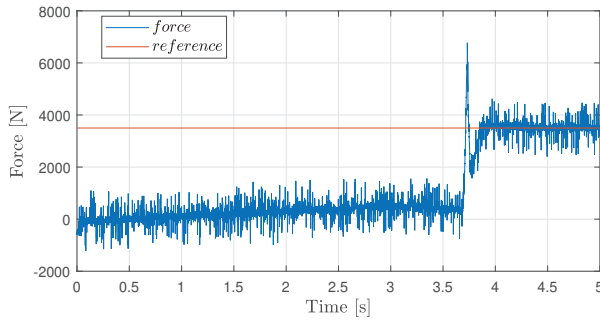

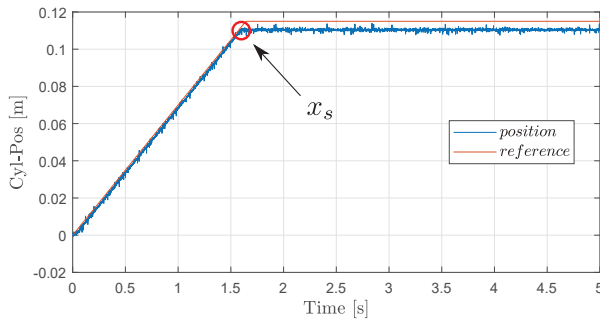Fig. 7: Measured load force and reference for 3500N

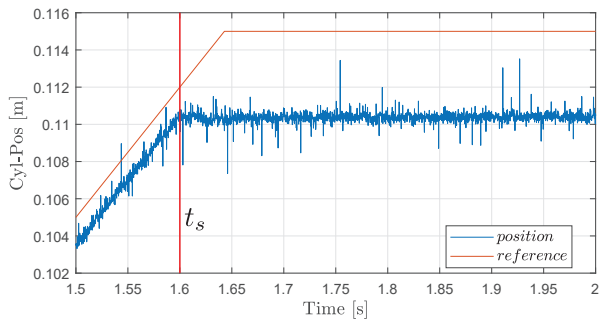Fig. 8: Measured cylinder position and reference for ramp with 0.07m/s slope

Fig. 9: Outtake of measured position and reference of ramp with slope of 0.07m/s

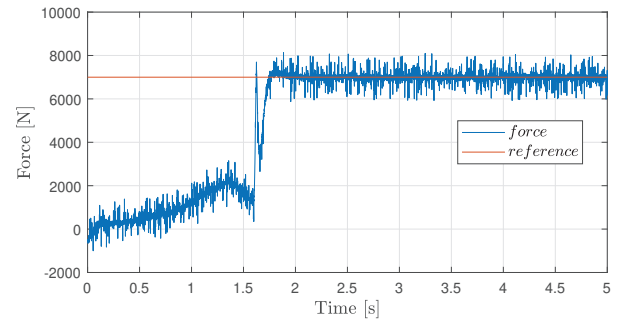increase of the measured force can be observed for both

Fig. 10: Measured load force and reference for 7000N

cases. Surpassing the threshold of $3500N$ triggers the event switching from the position to force control.

After a short transient the system reaches steady-state, holding a constant force against the hard stop for both cases according to their references. This also confirms, that the optimized gains are equally valid for varying reference signals. The validity of the simulation model and optimization routine is confirmed by determined gain factors equally suitable set for both simulated and real (measurement) control response. Taking a closer look at the position, exemplary for the ramp with a slope of $0.07m/s$ as shown in Fig. 9, it can be also observed that the cylinder is marginally penetrating into the hard stop around $t_s = 1.6s$, where the initial peak of the force is generated. This minimal penetration and well-matched transient to the force control response argues in favor of the designed event-based switching strategy.

V. SUMMARY

The state-space model of a hydraulic cylinder affine in control and states was expanded. Based on the identified dead-zone, a pre-compensator was designed and an integral-error-state-feedback controller implemented. The proposed approach realizes a closed-loop system capable of switching automatically between the position and force regulation depending on a measured mechanical resistance of environment. The trigger event initializing the switching from position to force control was introduced and the control gains for both integrator and state-feedback were found using optimization routines of position and force controls. A low-pass filter was added to the control signal while maintaining the systems overall fast response. Most important that a unified state feedback control structure has been developed equally suitable for both position and force control and well-matched switch between them. Real system experiments were performed and evaluated confirming efficiency of the proposed control approach and accuracy of the simulation model.

ACKNOWLEDGMENT

References

[1] G. Liu and S. Daley, "Optimal-tuning nonlinear PID control of hydraulic systems," *Control Engineering Practice*, vol. 8, no. 9, pp. 1045–1053, 2000.

[2] Bin Yao, Fanping Bu, J. Reedy, and G.-C. Chiu, "Adaptive robust motion control of single-rod hydraulic actuators: theory and experiments," *IEEE/ASME Transactions on Mechatronics*, vol. 5, no. 1, pp. 79–91, 2000.

[3] M. Ruderman, D. Weigel, F. Hoffmann, and T. Bertram, "Extended SDRE control of 1-DOF robotic manipulator with nonlinearities." Proc. 18th IFAC World Congress, 2011.

[4] S. Koch and M. Reichhartinger, "Observer-based sliding mode control of hydraulic cylinders in the presence of unknown load forces," *Elektrotechnik und Informationstechnik*, vol. 133, no. 6, pp. 253–260, 2016.

[5] C. Vazquez, S. Aranovskiy, L. Freidovich, and L. Fridman, "Second order sliding mode control of a mobile hydraulic crane," in *53rd IEEE Conference on Decision and Control*, 2014, pp. 5530–5535.

[6] A. Alleyne and R. Liu, "A simplified approach to force control for electro-hydraulic systems," *Control Engineering Practice*, vol. 8, no. 12, pp. 1347–1356, 2000.

[7] N. Niksefat and N. Sepehri, "Design and experimental evaluation of a robust force controller for an electro-hydraulic actuator via quantitative feedback theory," *Control Engineering Practice*, vol. 8, no. 12, pp. 1335–1345, 2000.

[8] J. Komsta, N. van Oijen, and P. Antoszkiewicz, "Integral sliding mode compensator for load pressure control of die-cushion cylinder drive," *Control Engineering Practice*, vol. 21, no. 5, pp. 708–718, 2013.

[9] S. Katsura, Y. Matsumoto, and K. Ohnishi, "Analysis and experimental validation of force bandwidth for force control," *IEEE Transactions on Industrial Electronics*, vol. 53, no. 3, pp. 922–928, 2006.

[10] O. Khatib, "A unified approach for motion and force control of robot manipulators: The operational space formulation," *IEEE Journal on Robotics and Automation*, vol. 3, no. 1, pp. 43–53, 1987.

[11] M. H. Raibert and J. J. Craig, "Hybrid Position/Force Control of Manipulators," *Journal of Dynamic Systems, Measurement, and Control*, vol. 103, no. 2, p. 126, 1981.

[12] W.-H. Zhu, S. Salcudean, S. Bachmann, and P. Abolmaesumi, "Motion/force/image control of a diagnostic ultrasound robot," in *Proceedings ICRA. Millennium Conference. IEEE International Conference on Robotics and Automation. Symposia Proceedings*, vol. 2, 2000, pp. 1580–1585.

[13] G. Roppenecker, "State Feedback Control of Linear Systems — a Renewed Approach," *at - Automatisierungstechnik*, vol. 57, no. 10, 2009.

[14] H. C. Pedersen and T. O. Andersen, "Pressure Feedback in Fluid Power Systems—Active Damping Explained and Exemplified," *IEEE Transactions on Control Systems Technology*, vol. 26, no. 1, pp. 102–113, 2018.

[15] J. K. Sørensen, M. R. Hansen, and M. K. Ebbesen, "Novel concept for stabilising a hydraulic circuit containing counterbalance valve and pressure compensated flow supply," *International Journal of Fluid Power*, vol. 17, no. 3, pp. 153–162, 2016.

[16] M. Ruderman, "Full- and reduced-order model of hydraulic cylinder for motion control," in *43rd Annual Conference of the IEEE Industrial Electronics Society*, 2017, pp. 7275–7280.

[17] P. Pasolli and M. Ruderman, "Linearized Piecewise Affine in Control and States Hydraulic System: Modeling and Identification." IECON2018 - 44th Annual Conference of the IEEE Industrial Electronics Society, 2018.

[18] M. Ruderman, "Computationally Efficient Formulation of Relay Operator for Preisach Hysteresis Modeling," *IEEE Transactions on Magnetics*, vol. 51, no. 12, pp. 1–4, 2015.